Photoacoustics 16 (2019) 100148

Contents lists available at ScienceDirect

Photoacoustics

journal homepage: www.elsevier.com/locate/pacs

Single-shot linear dichroism optical-resolution photoacoustic microscopy

Yingying Zhou[a,b,c,1], Jiangbo Chen[b,d,1], Chao Liu[b,d], Chengbo Liu[e], Puxiang Lai[a,c,*], Lidai Wang[b,d,**]

[a] Department of Biomedical Engineering, The Hong Kong Polytechnic University, Hong Kong
[b] Department of Biomedical Engineering, City University of Hong Kong, Hong Kong
[c] The Hong Kong Polytechnic University Shenzhen Research Institute, Shenzhen, China
[d] City University of Hong Kong Shenzhen Research Institute, Shenzhen, China
[e] Research Laboratory for Biomedical Optics and Molecular Imaging, Shenzhen Institutes of Advanced Technology, Chinese Academy of Sciences, Shenzhen, 518055, China

ARTICLE INFO

Keywords:
Linear dichroism
Photoacoustic microscopy
Polarization

ABSTRACT

Dichroism is a material property that causes anisotropic light-matter interactions for different optical polarizations. Dichroism relates to molecular types and material morphology and thus can be used to distinguish different dichroic tissues. In this paper, we present single-shot dichroism photoacoustic microscopy that can image tissue structure, linear dichroism, and polarization angle with a single raster scanning. We develop a fiber-based laser system to split one laser pulse into three with different polarization angles, sub-microseconds time delay, and identical pulse energy. A dual-fiber optical-resolution photoacoustic microscopy system is developed to acquire three A-lines per scanning step. In such a way, dichroism imaging can achieve the same speed as single-wavelength photoacoustic microscopy. Moreover, the three polarized pulses originate from one laser pulse, which decreases pulse energy fluctuations and reduces dichroism measurement noise by ~35 %. The new dichroism photoacoustic imaging technique can be used to image endogenous or exogenous polarization-dependent absorption contrasts, such as dichroic tumor or molecule-labeled tissue.

1. Introduction

Dichroism refers to anisotropic optical absorption property for different light polarizations. This property closely relates to molecular type and alignment. Dichroism can be determined via measuring absorption of different polarized irradiations with respect to the molecular or structural axis [1,2]. Dichroism detection can probe molecular types and structures of some biopolymers (such as protein and DNA) and synthetic polymers [3–6].

As an emerging optical imaging technique, photoacoustic (PA) tomography has seen a wide range of applications, including imaging dichroism in biological tissue. PA imaging also shows great potentials to provide multiple optical properties by being integrated with other optical modalities [7–9]. PA signal is proportional to absorbed optical energy [10–15] and, thus, provides a sensitive approach to measure dichroism. Dichroism-sensitive optical-resolution photoacoustic microscopy (OR-PAM) was first reported by Hu et al. [16]. In Hu's work, the OR-PAM system detects linear dichroism of amyloid plaques. An electro-optical modulator (EOM) alternates two perpendicularly polarized excitation beams pulse by pulse. While promising, two polarized beam is not enough to fully quantify the linear dichroism. In addition, the delay time between the two perpendicularly-polarized pulses is the laser pulse repetition time. The misalignment between the two polarizations is half step size, which may cause errors in dichroism imaging [17,18]. Qu et al. realized dichroism imaging in photoacoustic computed tomography (PACT) [19]. The polarization directions of dichroic materials, i.e., linear polarizers and bovine tendons, were successfully identified at depths of several transport mean free paths. Zhang et al. [20] developed a quantitative method to determine the dichroism from the anisotropy value. Both methods rotate a half-wave plate (HWP) to control the laser polarization and are time-consuming. This may be problematic in high-speed imaging.

Here, we develop a new OR-PAM technique that can measure linear dichroism in a single shot. The fast polarization measurement reduces misalignment among different polarized excitations, especially in fast scanning OR-PAM. In addition, the three different polarized laser pulses are generated from a single laser pulse, significantly reducing the energy fluctuation between the three pulses.

* Corresponding author at: Department of Biomedical Engineering, The Hong Kong Polytechnic University, Hong Kong.
** Corresponding author at: Department of Biomedical Engineering, City University of Hong Kong, Hong Kong.
E-mail addresses: puxiang.lai@polyu.edu.hk (P. Lai), lidawang@cityu.edu.hk (L. Wang).
[1] These authors contributed equally to this work.

https://doi.org/10.1016/j.pacs.2019.100148
Received 4 September 2019; Received in revised form 7 November 2019; Accepted 8 November 2019
Available online 19 November 2019

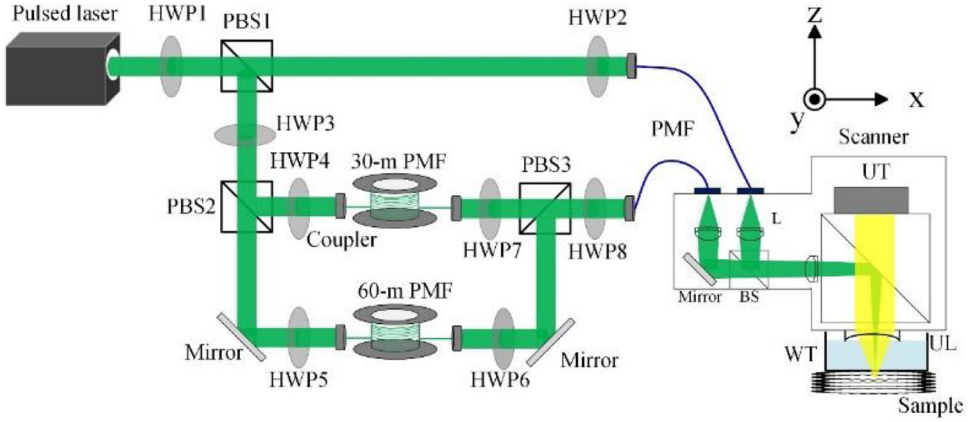

Fig. 1. Schematic of the dual-fiber single-shot dichroism OR-PAM system. BS, beamsplitter; HWP, halfwave plate; L, lens; PBS, polarizing beamsplitter; PMF, polarization-maintaining fiber; UL, ultrasound lens; UT, ultrasound transducer; WT, water tank.

2. Materials and methods

2.1. System setup

A linear dichroism OR-PAM system is shown in Fig. 1. A 532-nm pulsed laser (7 ns pulse width, linear polarization, VPFL-G-20, Spectra-Physics) is used as the photoacoustic excitation source. The output laser beam is split into three paths using two sets of polarizing beam splitters (PBS1 and PBS2) and halfwave plates (HWP1 and HWP3). The halfwave plates adjust the energy ratio among the paths. One laser path is delivered to an OR-PAM probe via a 2-m polarization-maintaining fiber (PMF, single mode, P1-488PM-FC-2, Thorlabs). The other two paths go through two polarization maintaining fibers (PMF, 30-m and 60-m long, respectively, single mode, HB450-SC, Fibercore) to generate different time delays. Then the two delayed paths are combined at a polarizing beamsplitter (PBS3) and delivered to the OR-PAM probe via another 2-m PMF (single mode, P1-488PM-FC-2, Thorlabs). Four halfwave plates (HWP2, HWP4, HWP5 and HWP8) are used to make sure the laser polarizations are aligned with the fast or slow axis of the polarization-maintaining fibers. Two halfwave plates (HWP6 and HWP7) are used to ensure that the laser beams are reflected or transmitted through PBS3 with high efficiency. The polarization directions of the two delayed paths are aligned with the fast and slow axes of the 2-m PMF, respectively. At the output end, the two 2-m PMFs are connected to the probe with two fiber adapters, and the angle between the fast axes of the two 2-m PMFs is 45°, so that we obtain three laser pulses with three different polarizations: 0°, 45°, and 90°. The three laser pulses have ~150-ns time interval and unchanged pulse energy ratio among them. In the imaging probe, the two laser beams from the fibers are collimated with an achromatic lens (AC064-013-A, Edmund) and then combined with a beamsplitter. Another achromatic lens (AC064-013-A, Edmund) focuses the combined beam. Then the focused beam is reflected in an optical/acoustic beam combiner (two prisms, PS910 and MRA10-F01 from Thorlabs Inc, glued together with NOA 61 from Norland Products, Inc.) [21], transmits through an ultrasonic lens, and illuminates the sample. Optically induced ultrasonic waves are collected by the ultrasonic lens, transmit through the optical/acoustic beam combiner, and are received by a 50-MHz piezoelectric transducer (V214-BC-RM, Olympus-NDT). Optical excitations from the two fibers are both aligned with the acoustic detection coaxially and confocally to maximize the detection sensitivity. This OR-PAM system acquires three A-lines with different polarized excitations at every scanning step. Raster scanning the PA probe allows for acquiring volumetric images.

2.2. Principle

Principle of the linear dichroism measurement is presented as follows. In linear photoacoustic range, the initial pressure can be expressed as [22–24]

$$p = \Gamma \eta_{th} \mu_a F, \tag{1}$$

where Γ is the Grueneisen parameter, η_{th} is the heat conversion efficiency, μ_a is the absorption coefficient, and F is the optical fluence. If the sample is dichroic, μ_a varies with the excitation polarization angle. For dichroic samples, assuming the optical axis orientation is θ, the polarization angle of light is φ. The μ_a depends on θ and φ as [16]

$$\mu_a(\theta,\varphi) = \frac{\mu_p + \mu_v}{2} + \frac{\mu_p - \mu_v}{2}\cos(2\varphi\text{-}2\theta) \tag{2}$$

where $\mu_a(\theta, \varphi)$ is the absorption coefficient when optical axis for target is θ and the polarized angle for light is φ. μ_p and μ_v are the optical absorption coefficient of the direction parallel with and perpendicular to the optical axis, respectively.

If we measure PA signals with three linear polarized pulses at 0°, 45° and 90°, we obtain

$$\begin{cases} p(\theta,0^o) = \Gamma\eta_{th}F\left[\dfrac{\mu_p+\mu_v}{2} + \dfrac{\mu_p-\mu_v}{2}\cos(0^o - 2\theta)\right] \\ p(\theta,45^o) = \Gamma\eta_{th}F\left[\dfrac{\mu_p+\mu_v}{2} + \dfrac{\mu_p-\mu_v}{2}\cos(90^o - 2\theta)\right] \\ p(\theta,90^o) = \Gamma\eta_{th}F\left[\dfrac{\mu_p+\mu_v}{2} + \dfrac{\mu_p-\mu_v}{2}\cos(180^o - 2\theta)\right] \end{cases}, \tag{3}$$

For simplicity, we let the three pulses have the same fluence. The dichroism is defined as $|(\mu_p - \mu_v)/(\mu_p + \mu_v)|$ [16]. Solving Eq. (3), we can determine the dichroism and polarization angle from the three PA measurements.

$$\theta = \frac{\arccos\left[\frac{p(\theta,0^o) - p(\theta,90^o)}{(2\times[(p(\theta,0^o) - p(\theta,45^o))^2 + (p(\theta,90^o) - p(\theta,45^o))^2])^{\frac{1}{2}}}\right]}{2}, \tag{4}$$

3. Results and discussion

3.1. Comparison between a linear polarizer and a black ink sample

Fig. 2 shows dichroism OR-PAM of a linear polarizer (Jiateng Video equipment Ltd China) and a black ink sample (unpolarized). Fig. 2a shows the PA images at three polarization angles. The upper row is the results from the linear polarizer sample, whose polarization angle is 135°. The lower row is the black ink sample. The linear polarizer results show obvious different PA intensities at different polarized excitations. The PA intensity at 45° excitation is lower than the other two, and the PA images at 0° and 90° excitations are nearly the same. Because the

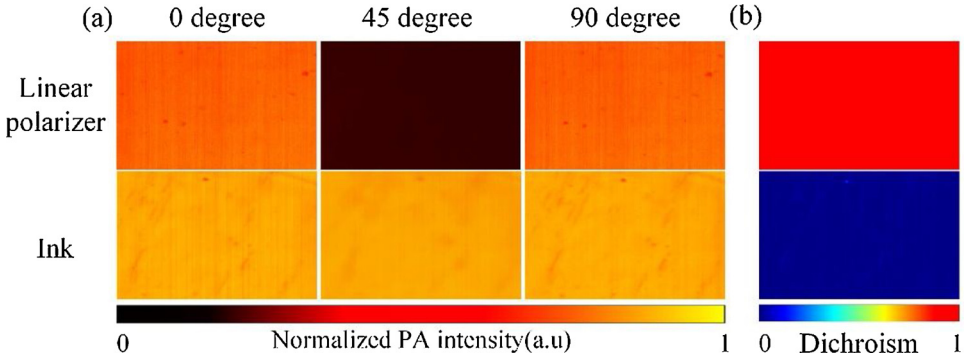

Fig. 2. (a) Linear polarizer (upper) and black ink (lower) images at 0°, 45°, and 90°. (b) Calculated dichroism of the linear polarizer (upper) and the black ink (lower) samples.

black ink has no dichroism, the PA images shows no obvious differences at different polarized light excitations. Dichroisms are calculated and shown in Fig. 2b. The averaged dichroism value for the linear polarizer is 0.96 ± 0.003, and the value for the black ink sample is nearly 0. We validate the dichroism of the linear polarizer in transmission mode using a power meter. The extinction ratio of the polarizer equals to 0.99, which is close to the PA imaging result.

3.2. Phantom experiment

To verify the dichroism imaging, three linear polarizers are positioned in different angles, as shown in Fig. 3. Fig. 3a shows three PA images acquired with three polarized light excitations. The polarizer gives strongest PA signals when its polarization angle aligns with the polarization angle of the excitation light. Fig. 3b shows the computed dichroism of the three linear polarizers. As expected, their dichroism is the same regardless their orientations. Fig. 3c shows the computed polarization angles θ according to Eq. (4). These results demonstrate that our single-shot OR-PAM can image dichroism correctly. An alternative approach is to measure the dichroism from independent pulses, such as using an EOM to switch between two different polarized laser beams [14]. Compared with the EOM-based method, our approach measures three PA signals originating from one laser pulse and thus can fully quantify the linear dichroism. In addition, the three laser pulses have reduced pulse energy fluctuations and misalignment. The standard deviation of the dichroism results from our approach is 0.0455, 35 % less than the other approach.

3.3. Biological tissue experiment

We further demonstrate single-shot dichroism OR-PAM with biological tissue. Congo Red dye is a dichroic molecule. In experiment, 0.01 g Congo Red (C8450, Solarbio) was dissolved in 0.2 ml deionized water, and was used to dye a ~200-μm-thick chicken breast tissue sample. First, we tested photo bleaching rate of the labelled sample in OR-PAM imaging. The laser pulse energy in experiment was 30 nJ. The averaged PA amplitude decreases ~58 % per one million pulsed excitations. For raster scanning, the laser spot size is 5 μm and the step size is 1.25 μm. Thus, the sample bleaching at one spot is 0.002784 % for three pulsed excitations. Thus, photo bleaching causes negligible influence to the single-shot dichroism imaging.

Fig. 4a shows a maximum-amplitude-projected PA image of the chicken breast sample. The polarization angle of the excitation light for this image is 0°. The laser repetition rate is 8 kHz for each polarization

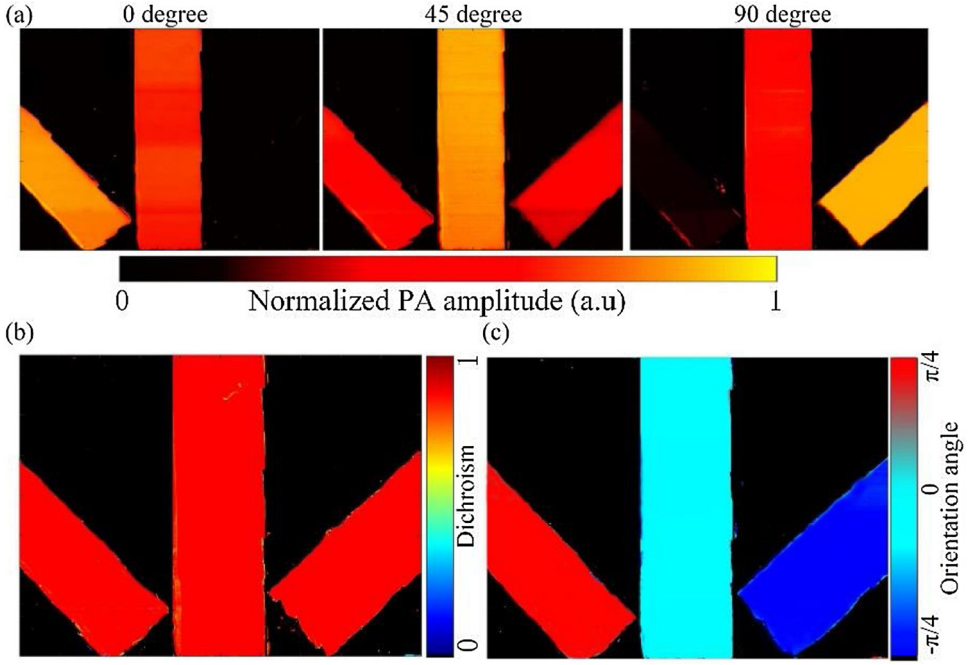

Fig. 3. (a) PA images of three linear polarizers excited with polarized light at 0°, 45°, and 90°. (b) Calculated dichroism image of the three linear polarizers. (c) Calculated polarization angle of the three linear polarizers.

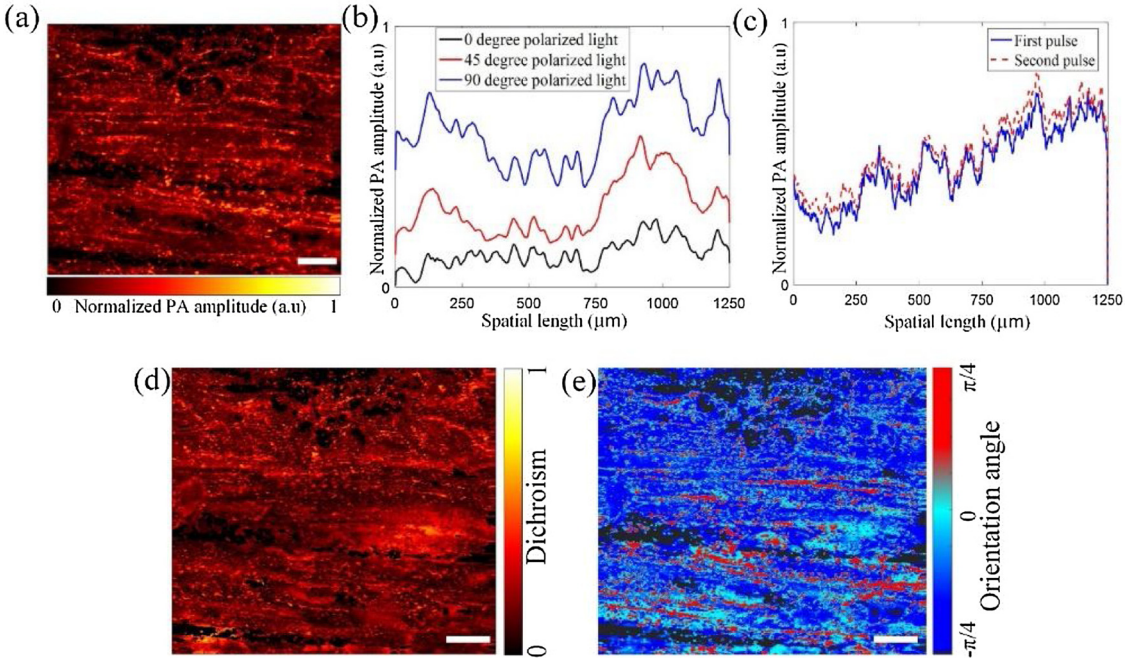

Fig. 4. (a) OR-PAM of a Congo-Red-dyed chicken breast tissue sample. (b) Averaged PA amplitudes excited with different linear polarization light at 0°, 45°, and 90°. (c) Test of Grueneisen relaxation effect. Averaged PA amplitudes excited with two non-polarized pulses. Time delay between the two pulses is 150 ns. (d) Calculated dichroism image. (e) Calculated polarization angle image. (scale bar: 150 μm).

angle. The scanning step size is 1.25 μm, and the field of view is 1.25×1.25 mm^2. Fig. 4b shows the spatial profile of averaged PA amplitudes along the B-scan direction at three excitation polarization angles. Dichroism of the sample causes dramatic differences among the three images. Because the time delay among the three pulses is sub-microseconds, the Grueneisen parameter might be changed due to local heating [22–24]. To exclude this possibility, we use two non-polarized laser pulses to excite the sample. The two pulses have the same pulse energy of 30 nJ. The time delay between them is ~150 ns. As seen in Fig. 4c, the PA amplitude variation associated with the Grueneisen effect does exist, as the second PA amplitude increases ~3 % due to local heating. Nevertheless, compared with polarization difference-induced difference (~25 % variation for each different polarization) shown in Fig. 4b, the Grueneisen effect causes ~12 % error in the dichroism measurement. In the future, this error may be reduced via increasing the time delay among the three pulses or using less pulse energy. Fig. 4d and e show the dichroism and polarization angle distributions of the Congo Red-dyed chicken breast tissue sample. The dichroism of the sample is relatively uniform due to the use of the same dye. The polarization angle distribution, however, shows more variations due to the inhomogeneities of muscle fiber directions.

4. Conclusion

We present the development of a single-shot linear dichroism OR-PAM. To quantify the linear polarization, the OR-PAM system excites the sample with three laser pulses at different polarization angles. One laser pulse output of a fiber-based laser source is split into three with different polarization angles and different time delays. This approach provides stable energy ratio among the three pulses and thus can reduce the noise in dichroism imaging. Polarization switch is implemented via fiber delay. This offers sub-microseconds polarization switching and thus can reduce misalignment among different polarizations, even in fast scanning. The three laser pulses are delivered to a dual-fiber OR-PAM probe for PA imaging. Experimental results show that dichroism OR-PAM can quantify dichroism and polarization angle in a single raster scanning. This technical advancement offers a new polarization contrast to optical-resolution photoacoustic microscopy and may extend it to broader preclinical and clinical applications.

Declaration of Competing Interest

C.L. and L.W. have a financial interest in PATech Limited, which, however, did not support this work.

Acknowledgment

The work is supported in part by the Hong Kong Research Grant Council (25204416, 21205016, 11215817, and 11101618), the National Natural Science Foundation of China (81671726, 81930048 and 81627805), the Shenzhen Science and Technology Innovation Commission (JCYJ20170818104421564, JCYJ20160329150236426, and JCYJ20170413140519030), and the Hong Kong Innovation and Technology Commission (ITS/022/18).

References

[1] B. Norden, M. Kubista, T. Kurucsev, Linear dichroism spectroscopy of nucleic-acids, Q. Rev. Biophys. 25 (1) (1992) 51–170.
[2] B.M. Bulheller, A. Rodger, J.D. Hirst, Circular and linear dichroism of proteins, Phys. Chem. Chem. Phys. 9 (17) (2007) 2020–2035.
[3] J.S. Qiao, X.H. Kong, Z.X. Hu, F. Yang, W. Ji, High-mobility transport anisotropy and linear dichroism in few-layer black phosphorus, Nat. Commun. 5 (2014).
[4] B. Norden, Applications of linear dichroism spectroscopy, Appl. Spectrosc. Rev. 14 (2) (1978) 157–248.
[5] K. Razmkhah, N.P. Chmel, M.I. Gibson, A. Rodger, Oxidized polyethylene films for orienting polar molecules for linear dichroism spectroscopy, Analyst 139 (6) (2014) 1372–1382.
[6] G.Z. Zhang, J. Li, P. Cui, T. Wang, J. Jiang, O.V. Prezhdo, Two-dimensional linear dichroism spectroscopy for identifying protein orientation and secondary structure composition, J. Phys. Chem. Lett. 8 (5) (2017) 1031–1037.
[7] Z.J. Chen, S.H. Yang, D. Xing, Optically integrated trimodality imaging system: combined all-optical photoacoustic microscopy, optical coherence tomography, and fluorescence imaging, Opt. Lett. 41 (7) (2016) 1636–1639.
[8] C. Liu, J. Liao, L. Chen, J. Chen, R. Ding, X. Gong, C. Cui, Z. Pang, W. Zheng, L. Song, The integrated high-resolution reflection-mode photoacoustic and fluorescence confocal microscopy, Photoacoustics 14 (2019) 12–18.
[9] M. Seeger, A. Karlas, D. Soliman, J. Pelisek, V. Ntziachristos, Multimodal optoacoustic and multiphoton microscopy of human carotid atheroma, Photoacoustics 4

(3) (2016) 102–111.
[10] L.H.V. Wang, S. Hu, Photoacoustic Tomography: In vivo imaging from organelles to organs, Science 335 (6075) (2012) 1458–1462.
[11] M.H. Xu, L.H.V. Wang, Photoacoustic imaging in biomedicine, Rev. Sci. Instrum. 77 (4) (2006).
[12] J. Xia, J.J. Yao, L.V. Wang, Photoacoustic tomography: principles and advances, Prog Electromagn Res 147 (2014) 1–22.
[13] F. Cao, Z.H. Qiu, H.H. Li, P.X. Lai, Photoacoustic imaging in oxygen detection, Appl Sci-Basel 7 (12) (2017).
[14] Y.J. Liu, H.H. Liu, H.X. Yan, Y.C. Liu, J.S. Zhang, W.J. Shan, P.X. Lai, H.H. Li, L. Ren, Z.J. Li, L.M. Nie, Aggregation-induced absorption enhancement for deep near-infrared II photoacoustic imaging of brain gliomas in vivo, Adv. Sci. 6 (8) (2019).
[15] X. Huang, W. Shang, H. Deng, Y. Zhou, F. Cao, C. Fang, P. Lai, J. Tian, Clothing spiny nanoprobes against the mononuclear phagocyte system clearance in vivo: photoacoustic diagnosis and photothermal treatment of early stage liver cancer with erythrocyte membrane-camouflaged gold nanostars, Appl. Mater. Today (2019).
[16] S. Hu, K. Maslov, P. Yan, J.M. Lee, L.V. Wang, Dichroism optical-resolution photoacoustic microscopy, Proc. SPIE. Int. Soc. Opt. Eng. 8223 (2012).
[17] Y.Z. Liang, L. Jin, B.O. Guan, L.D. Wang, 2 MHz multi-wavelength pulsed laser for functional photoacoustic microscopy, Opt. Lett. 42 (7) (2017) 1452–1455.
[18] T. Wang, N. Sun, R. Cao, B. Ning, R. Chen, Q. Zhou, S. Hu, Multiparametric photoacoustic microscopy of the mouse brain with 300-kHz A-line rate, Neurophotonics 3 (4) (2016) 045006.
[19] Y. Qu, L. Li, Y.C. Shen, X.M. Wei, T.T.W. Wong, P. Hu, J.J. Yao, K. Maslov, L.H.V. Wang, Dichroism-sensitive photoacoustic computed tomography, Optica 5 (4) (2018) 495–501.
[20] Z.H. Zhang, Y.J. Sh, L.Z. Xiang, D. Xing, Polarized photoacoustic microscopy for vectorial-absorption-based anisotropy detection, Opt. Lett. 43 (21) (2018) 5267–5270.
[21] L.D. Wang, K. Maslov, J.J. Yao, B. Rao, L.H.V. Wang, Fast voice-coil scanning optical-resolution photoacoustic microscopy, Opt. Lett. 36 (2) (2011) 139–141.
[22] L.D. Wang, C. Zhang, L.H.V. Wang, Grueneisen relaxation photoacoustic microscopy, Phys. Rev. Lett. 113 (17) (2014).
[23] P.X. Lai, L.D. Wang, J.W. Tay, L.H.V. Wang, Photoacoustically guided wavefront shaping for enhanced optical focusing in scattering media, Nat. Photonics 9 (2) (2015) 126–132.
[24] L.D. Wang, K. Maslov, L.H.V. Wang, Single-cell label-free photoacoustic flowoxigraphy in vivo, P Natl Acad Sci USA 110 (15) (2013) 5759–5764.

Liu Chao is a Ph.D. candidate student from Biomedical Engg Department in City University of Hong Kong. He received Bachelor degree from Xi'an Jiaotong University, and Master degree from Hong Kong University of Science and Technology. His research emphasis focuses on photoacoustic microscopy and biophotonics.

Chengbo Liu received both his Ph.D and Bachelor degree from Xi'an Jiaotong University, each in 2012 in Biophysics and 2007 in Biomedical Engineering. During his Ph.D. training, he was very grateful to be supported by China Scholarship Council for doing two years visiting research at Duke University. His previous research has been mainly focused on tissue spectroscopy and its application in early cancer diagnosis. Now he is an associate professor at SIAT, working on macroscopic photoacoustic imaging and its translational research. He has published more than 10 SCI journal papers (5 first author papers), applied for 5 patents so far, and is currently a member of IEEE, OSA, and SPIE. Besides academic research, Chengbo also enjoys playing soccer and a variety of other sport activities.

Chen Jiangbo is a PhD student at the Department of Biomedical Engineering, City University of Hong Kong. He received Bachelor degree from the Northeast Forestry University, and received Master degrees from Harbin institute of technology. His research focuses on photoacoustic imaging.

Lidai Wang received the Bachelor and Master degrees from the Tsinghua University, Beijing, and received the Ph.D. degree from the University of Toronto, Canada. After working as a postdoctoral research fellow in the Prof Lihong Wang's group, he joined the City University of Hong Kong in 2015. His research focuses on biophotonics, biomedical imaging, wavefront engineering, instrumentation and their biomedical applications. He has invented single-cell flowoxigraphy (FOG), ultrasonically encoded photoacoustic flowgraphy (UE-PAF) and nonlinear photoacoustic guided wavefront shaping (PAWS). He has published more 30 articles in peer-reviewed journals and has received four best paper awards from international conferences.

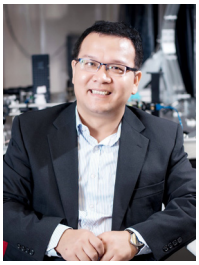

Dr. Puxiang Lai received his Bachelor from Tsinghua University in 2002, Master from Chinese Academy of Sciences in 2005, and PhD from Boston University in 2011. After that, he joined Dr Lihong Wang's lab in Washington University in St. Louis as a Postdoctoral Research Associate. In September 2015, he joined Department of Biomedical Engineering at the Hong Kong Polytechnic University. Dr. Lai's research focuses on the synergy of light and sound as well as its applications in biomedicine. His research has fueled more than 40 top journal publications, such as *Nature Photonics* and *Nature Communications*.

Yingying ZHOU is a PhD student at the Department of Biomedical Engineering, The Hong Kong Polytechnic University. She received Bachelor degree from the SUN YAT-SEN UNIVERSITY. Her research focuses on photoacoustic microscopy and its applications.